Correct self-assembling of spatial frequencies in super-resolution synthetic aperture digital holography

Melania Paturzo and Pietro Ferraro*

CNR–Istituto Nazionale di Ottica Applicata, via Campi Flegrei 34, 80078 Pozzuoli (NA) Italy
**Corresponding author: pietro.ferraro@inoa.it*

Received June 12, 2009; revised October 14, 2009; accepted October 14, 2009;
posted October 27, 2009 (Doc. ID 112752); published November 20, 2009

Synthetic aperture enlargement is obtained, in lensless digital holography, by introducing a diffraction grating between the object and the CCD camera with the aim of getting super-resolution. We demonstrate here that the spatial frequencies are naturally self-assembled in the reconstructed image plane when the NA is increased synthetically at its maximum extent of three times. By this approach it possible to avoid the use of the grating transmission formula in the numerical reconstruction process, thus reducing significantly the noise in the final super-resolved image. Demonstrations are reported in 1D and 2D with an optical target and a biological sample, respectively. © 2009 Optical Society of America

OCIS codes: 100.6640, 110.0180, 050.1950, 070.6020, 090.0090, 090.1760.

Digital holography (DH) in microscope configuration have been extensively adopted in many fields such as biology [1,2], 3D imaging [3], and particle analysis [4,5]. An important configuration is the lensless one, which offers high simplicity with a reasonably magnification, which is useful in microscopy [5]. The resolution of an optical system is limited by its NA that in lessless DH is given by the lateral dimension of the detector. The finite aperture of the imaging system prevents the sensor from collecting light scattered at large angles. Therefore, depending on the object, a certain amount of information is missed into the recorded holograms, thus leading to a reconstructed image with a band-limited spatial frequency domain. Various strategies have been tested to synthetically increase the NA in order to get super-resolution [6,7]. The NA was increased recording nine holograms with a CCD in different positions and recombining them in a synthetic hologram [8]. Super-resolution was achieved by rotating the sample in its plane [9] or in respect to the optical axis [10] and recording a digital hologram for each position in order to capture the diffraction field along different directions. Recently new approaches to get super-resolved images has been demonstrated [11–14]. Super-resolved images can be obtained simply by using 1D diffraction grating [15] or a 2D tuneable phase grating [16] that allows one to collect parts of the light diffracted from the object that otherwise would fall outside the CCD. Different digital holograms, according to the grating geometry, are spatially multiplexed onto the same CCD array, and the super-resolved images are obtained by the numerical reconstruction, taking into account the transmission function of the grating (GTF). The main advantage of this method in respect to the others is that, by introducing the correct GTF into the reconstruction diffraction integral, the spatial frequencies of the objects are assembled together automatically without tedious numerical superimposing operations [8–13]. Nevertheless, the introduction of the GTF produces some deleterious numerical noise that affects the final super-resolved image.

Here we demonstrate that, when the NA improvement is exactly equal to three, it is not necessary to introduce the GTF in the numerical reconstruction. In fact, in this case the result is that the reconstructed images corresponding to the different diffraction orders are automatically and precisely superimposed. We show that it is possible to exploit the typical wrapping effect in the reconstructed image plane when the bandwidth of the image does not fit entirely into the reconstructed window. This method has two significant advantages. First, avoiding the use of the GTF the noise is reduced considerably. Second, there is no restriction in the object field of view. Strong field of view restrictions were necessary in our previous approach so that the different bandpass images, coming from the different diffraction orders, will not overlap in the image plane [16]. As to the used grating, in the first part of the Letter, we present the experimental validation of the proposed approach through a 1D resolution improvement, employing an amplitude grating with a pitch of 25 μm. In the second part, where we show a 2D super-resolved image of a biological sample, we used 2D amplitude gratings with the same pitch.

The sketch in Fig. 1 describes the object wave optical path during the recording [Fig. 1(a)] and the reconstruction processes [Fig. 1(b)]. The CCD records three spatially multiplexed holograms corresponding to three diffraction orders. Each hologram carries different information about the object. The hologram corresponding to the zero order contains the low-object frequencies, while the holograms corresponding to the first orders collects the rays scattered at wider angles carrying information about higher frequencies. Three distinct images corresponding to each hologram are numerically reconstructed, as shown in Fig. 1(b). Our aim is to assemble these three images in an appropriate way in order to get super-resolution. In Fig. 1 the black (blue online) squares in the CCD plane indicate the center of the

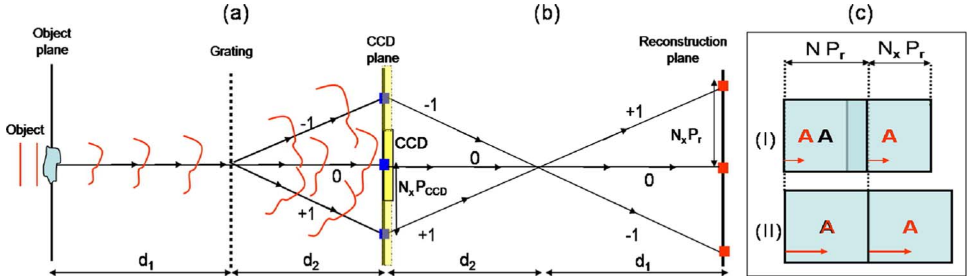

Fig. 1. (Color online) (a) DH setup with a grating, (b) geometric scheme of the reconstruction without a grating in self-assembling mode, (c) geometric scheme to show the automatic superimposition in the self-assembling mode.

three holograms, while the gray (red online) squares in the reconstruction plane are the center of the reconstructed images. The distance between two contiguous holograms is $N_xP_{\rm CCD}$, where $P_{\rm CCD}$ is the CCD pixel size and N_x is a real number, while the distance between two reconstructed images is N_xP_r, where P_r is the reconstruction pixel. When N_x is equal to N, that is, the number of CCD pixels, the relative distance among the three holograms is exactly equal to the lateral dimension of the CCD array (Fig. 1). Therefore, only when $N_x=N$, we obtain a resolution enhancement equal to three. By a simple geometrical computation, the distance between the zero and the first diffracted orders in the CCD plane is $\Delta x=\lambda d_2/p$, where p is the grating pitch and d_2 is the distance between the grating and the CCD. To obtain an NA improvement equal to three it is necessary to fulfill the condition $\Delta x=\mathrm{N}P_{\rm CCD}$; the distance d_2 has to be

$$d_2=\frac{pNP_{\rm CCD}}{\lambda}. \tag{1}$$

If d_2 does not match Eq. (1) exactly, we have $\Delta x=N_xP_{\rm CCD}$, and the improvement of the NA is given by $1+2(N_x/N)$ with $N_x\leqslant N$. Only if we get the resolution improvement of three is it possible to obtain at the same time an automatic self-assembling of the various spatial frequency of the objects in the reconstruction image plane. In Fig. 1(c) the geometric diagram is shown, concerning the reconstructed images, to explain how it happens. It results that the lateral distance between the three reconstruction images is equal to

$$\Delta\xi=N_x\mathrm{Pr}, \tag{2}$$

where $\mathrm{Pr}=d_1/d_2P_{\rm CCD}$ is the reconstruction pixel for the double-step reconstruction process we use [16,17]. In fact, all the reconstructions are obtained by the two-step process computing two Fresnel integrals: first we reconstruct the hologram in the grating plane, and then we propagate this complex field up to the object plane [16]. In the double-step reconstruction, the Pr depends only on the ratio d_1/d_2, while it does not depend on the distance $D=d_1+d_2$ between the object and the CCD, different from what occurs in a typical single-step Fresnel reconstruction process, where $\mathrm{Pr}=\lambda D/(NP_{\rm CCD})$. It is worth noting that in DH, when the reconstruction window is not large enough to contain the entire spatial frequency band of the object, the object signal is wrapped within the reconstruction window. In our case, the object lateral dimension is $(N+2N_x)\mathrm{Pr}$, while the reconstruction window is only $N\mathrm{Pr}$. In Fig. 1(c) (I) only the central and right reconstruction image windows are shown, corresponding to $(N+N_x)\mathrm{Pr}$. The left reconstructed image has been omitted for clarity. Letter A represents the central point of the field of view of each reconstructed hologram. In Fig. 1(c) (I), the portion of the right image that includes the gray (red online) letter A falls outside the reconstruction window and, therefore, is wrapped and re-enters in the reconstruction window from the left side. In this case the multiple reconstructed images are incorrectly superimposed in the reconstruction plane. Only when $N_x=N$ [as in Fig. 1(c) (II)], when the gray letter is perfectly superimposed to the black one, the reconstructed images, corresponding to the different diffraction orders, are automatically and perfectly superimposed. The fulfillment of the condition $N_x=N$ assures the self-assembling of the object spatial frequencies in the reconstructed plane and allows one to enhance the resolution with a factor of 3 without introducing the GTF in the diffraction propagation algorithm.

In Fig. 2 are shown different numerical reconstructions obtained for different values of the distance d_1 and d_2. The grating has a pitch of 25 μm; therefore, to fulfill the condition of Eq. (1), d_2 has to be 21 cm. Looking at Fig. 2, it is clear that only when $d_2=21$ cm the three reconstructions are superimposed. Moreover, we can assert that the value of distance d_1 does not affect the self-assembling properties but

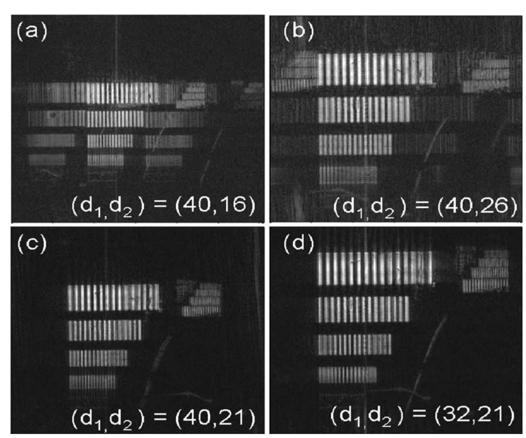

Fig. 2. Reconstructions adopting different values $(d1,d2)$. Spatial frequencies are wrongly assembled in (a) and (b) and are correct in (c) and (d).

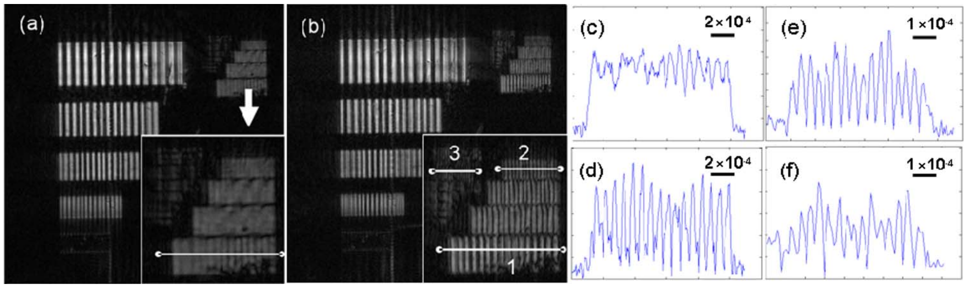

Fig. 3. (Color online) Reconstructions (a) without and (b) with the grating (super-resolved image). In (c) profile of the 100 μm along the line in the inset of (a) showing that the grating is not well resolved. (d), (e), and (f) Profiles of lines 1, 2, and 3 indicated in (b).

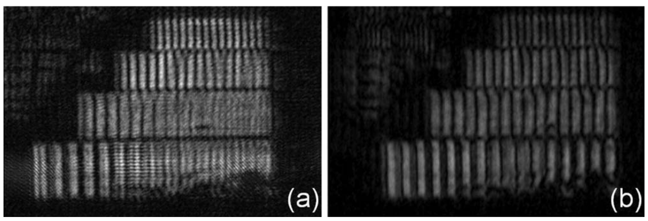

Fig. 4. (a) Super-resolved image obtained by the method in [15,16] and (b) by using self-assembling approach.

only the value of the pixel of reconstruction and, therefore, the field-of-view width. Fixing the values $(d_1 d_2)=(32,21)$ (units are centimeters), we measured the effective resolution improvement. Figures 3(a) and 3(b) show the numerical reconstructions without and with the grating in the setup. The profiles corresponding to the reticule with pitch of 100 μm (line 1) are shown in Figs. 3(c) and 3(d), respectively. Figures 3(e) and 3(f) show the profiles of the reticules with pitch of 50.14 μm (line 2) and 31.63 μm (line 3) obtained by the hologram recorded with the grating in the setup. The last one has approximately the same contrast of the grating with a pitch of 100 μm obtained by the reconstruction of the hologram acquired without the grating in the setup. Therefore, the resolution enhancement is effectively equal to three. Moreover, to show how the use of the GTF in the reconstruction process affect the image quality, a magnified view of a portion of the reconstructed target using the method that adopts the GTF [16] and by the self-assembling approach proposed here are shown in Figs. 4(a) and 4(b), respectively. It is clear that the noise introduced by the GTF hinders some relevant information in the super-resolved image.

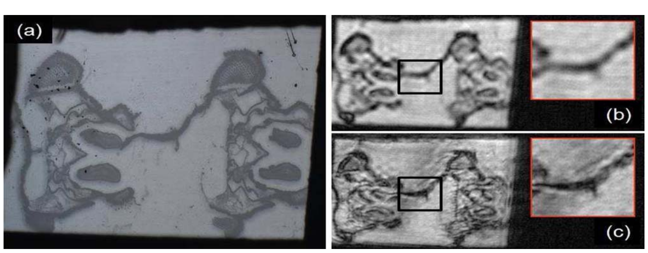

Fig. 5. (Color online) (a) Slice of fly's head eye at optical microscope, (b) DH reconstructed image without super-resolution, (c) super-resolved image.

Finally, we recorded a hologram of a biological sample, a slice of a fly's head. The image of the slice as it appears at an optical microscope is shown in Fig. 5(a). In this case a 2D grating was used. Therefore, the resolution increases three times along two directions. Figures 5(b) and 5(c) show the reconstructions of the holograms with and without the grating, respectively. The insets in Figs. 5(b) and 5(c) show how fine details of the object are clearly unresolved in the optical configuration without a grating, while they are visibly resolved with the 2D grating and self-assembling.

Research funded from the EU FP7/2007–2013, grant 216105. The authors thank A. Finizio and V. Guglielmotti.

References

1. B. Kemper and G. von Bally, Appl. Opt. **47**, A52 (2008).
2. P. Ferraro, D. Alfieri, S. De Nicola, L. De Petrocellis, A. Finizio, and G. Pierattini, Opt. Lett. **31**, 1405 (2006).
3. L. Xu, X. Peng, J. Miao, and A. K. Asundi, Appl. Opt. **40**, 5046 (2001).
4. F. Dubois, N. Callens, C. Yourassowsky, M. Hoyos, P. Kurowski, and O. Monnom, Appl. Opt. **45**, 864 (2006).
5. J. Garcia-Sucerquia, W. Xu, S. K. Jericho, P. Klages, M. H. Jericho, and H. J. Kreuzer, Appl. Opt. **45**, 836 (2006).
6. F. Le Clerc, M. Gross, and L. Collot, Opt. Lett. **26**, 1550 (2001).
7. R. Binet, J. Colineau, and J.-C. Lehureau, Appl. Opt. **41**, 4775 (2002).
8. J. H. Massig, Opt. Lett. **27**, 2179 (2002).
9. S. A. Alexandrov, T. R. Hillman, T. Gutzler, and D. D. Sampson, Phys. Rev. Lett. **97**, 168102 (2006).
10. Y. Kuznetsova, A. Neumann, and S. R. Brueck, Opt. Express **15**, 6651 (2007).
11. L. Martínez-León and B. Javidi, Opt. Express **16**, 161 (2008).
12. V. Mico, Z. Zalevsky, C. Ferreira, and J. García, Opt. Express **16**, 19260 (2008).
13. T. R. Hillman, T. Gutzler, S. A. Alexandrov, and D. D. Sampson, Opt. Express **17**, 7873 (2009).
14. P. Feng, X. Wen, and R. Lu, Opt. Express **17**, 5473 (2009).
15. C. Liu, Z. Liu, F. Bo, Y. Wang, and J. Zhu, Appl. Phys. Lett. **81**, 3143 (2002).
16. M. Paturzo, F. Merola, S. Grilli, S. De Nicola, A. Finizio, and P. Ferraro, Opt. Express **16**, 17107 (2008).
17. F. Zhang, I. Yamaguchi, and L. P. Yaroslavsky, Opt. Lett. **29**, 1668 (2004).